Neoclassical theory for rotation and impurity transport in tokamaks with neutral beam injection

Weston M. Stacey
Fusion Research Center, Georgia Institute of Technology, Atlanta, Georgia 30332-0225

(Received 26 May 2000; accepted 19 September 2000)

A self-consistent, first-principles neoclassical theory for rotation and impurity transport in tokamaks is presented. The implications of this theory for impurity transport in a tokamak are illustrated by a model problem calculation. © *2001 American Institute of Physics.* [DOI: 10.1063/1.1324664]

I. INTRODUCTION

While transport in tokamaks is generally thought to be dominated by anomalous effects, there is a growing body of evidence that under certain conditions neoclassical theory can account for many aspects of ion transport. For example, in enhanced reverse shear plasmas in the Tokamak Fusion Test Reactor[1,2] (TFTR) and negative central shear plasmas in DIII-D[3] turbulence is suppressed and the standard neoclassical expressions predict the measured ion thermal conductivity rather well. Calculations of momentum confinement time based on neoclassical gyroviscous theory have agreed,[4] rather well with measurements in several tokamaks. In *H*-mode (high confinement mode) plasmas in the Joint European Torus (JET), the measured value of radial impurity flow has been shown[5] to be in agreement with neoclassical theory, and neoclassical temperature gradient screening may explain the expulsion of carbon from the core in JET hot ion mode discharges.[5]

This apparent applicability of neoclassical theory to tokamak ion transport encourages us to assemble from previous work an internally self-consistent, first-principles neoclassical model for the investigation of impurity transport and plasma rotation. By ''internally self-consistent'' and ''first principles'' we mean that, within the context of the multifluid description of the plasma and the constitutive relations which we use, the various particle transport fluxes and flows, momentum transport fluxes, electric fields, and density asymmetries are all calculated on a consistent basis, without the need for external specification of any of the quantities involved. Internally self-consistent ''components'' for a neoclassical calculation of rotation and impurity transport have been developed in a series of papers; however, each of these component calculations requires external specification of some rotation velocity or cross-field momentum transport rate, and so is not fully ''first principles.'' Our objective in this paper is to assemble these various component calculations into a first-principles, internally self-consistent neoclassical calculation of rotation and impurity transport in tokamak plasmas. First, we will review the development of the component calculations.

The original neoclassical theory (e.g., Ref. 6), which treats the plasma as an isolated system with no external interactions, predicts the central accumulation of impurity ions in the absence of a radial temperature gradient or external source of particles and predicts the diminishment of this central accumulation in the presence of the usual negative radial temperature gradient (i.e., temperature screening). Ohkawa[7] was the first to point out the importance of taking into account the interaction of the plasma with external sources, noting that the momentum exchange with fast ions produced by neutral beam injection (NBI) could drive a radial transport flux of plasma ions which was inward when the magnetic field, current, and beam directions were parallel, and outward when one of these directions was antiparallel to the other two. Stacey and Sigmar[8] noted that the saturation of the rotation velocity in beam injected experiments implied a radial transport of momentum across flux surfaces, or a ''drag'' force proportional to the velocity acting to saturate the bulk rotation of particles on a flux surface. They found that the presence of this drag force enabled a leading order calculation of the radial electric field, that the momentum exchange between beam ions and plasma ions altered the plasma flows in the flux surface and the radial electric field, and that these effects produced radial transport fluxes of ions. Burrell, Ohkawa, and Wong[9] showed that an inertial effect produced by the beam-induced plasma rotation produced in turn a radial ion transport flux. These various effects were all embodied in the rotation and impurity transport theory of Stacey *et al.*,[10] which is internally self-consistent but requires external specification of the ''drag'' force which represents cross-field transport of toroidal momentum. This theory predicted that the net effect on impurity transport of NBI in model problems representative of then current tokamaks was to produce an outward impurity flux when the beam, magnetic field, and current directions were in parallel and an inward impurity flux when one of the directions was antiparallel to the other two.

In the meantime, a number of experiments were performed in ISX-B[11,12] (Impurity Studies Experiment B) and Princeton Large Torus[13,14] to investigate the effect of NBI direction on central impurity accumulation. These experimental results confirmed the qualitative theoretical prediction that accumulation of impurities in the center of these plasmas was substantially smaller when the magnetic field, beam, and plasma current were parallel than when one was antiparallel to the other two. These experiments were interpreted[15] in terms of the theory of Ref. 10.

The next step in the development of this extended neo-

classical theory for rotation and impurity transport was the association of the ''drag'' force, or cross-field transport of toroidal momentum, with the neoclassical gyroviscous stress by Stacey and Sigmar.[16] Evaluation of this gyroviscous stress requires calculation of the poloidal flows of impurities and main ions within the flux surface and calculation of the poloidal variation of the main ion and impurity densities over the flux surface. Stacey[17] developed an internally self-consistent model for the calculation of poloidal flows and density variations over the flux surface, but this model required external specification of the toroidal rotation. Stacey and Jackson[4] applied this model to calculate momentum confinement times which were in good agreement with measured values for a range of tokamak experiments (Asymmetric Divertor Experiment, DIII, ISX-B, JET, and TFTR).

Thus, the pieces of an internally self-consistent neoclassical model for rotation and impurity transport have been developed and individually tested by comparison with experiment, but the model has not heretofore been assembled into a single, fully ''first-principles'' computational package. The primary purpose of this paper is to do just that. Applications of the resulting computational package to illustrate its predictions under typical experimental conditions are a secondary purpose of the paper.

We note that a similar neoclassical computational model has been the subject of a parallel development by Hirshman and co-workers (e.g., Refs. 18 and 19).

II. THEORETICAL NEOCLASSICAL MODEL

A. Multifluid equations

The theoretical model is developed within the context of the multifluid particle and momentum balance equations

$$\nabla\cdot n_j\mathbf{v}_j=0 \tag{1}$$

and

$$n_j m_j(\mathbf{v}_j\cdot\nabla)\mathbf{v}_j+\nabla p_j+\nabla\cdot\pi_j=-n_j e_j\nabla\Phi+n_j e_j(\mathbf{v}_j\times\mathbf{B})+\mathbf{R}_j+\mathbf{M}_j, \tag{2}$$

where $\mathbf{M}$ is any external momentum input (e.g., from NBI) and the other symbols are standard. This multifluid model is supplemented by constitutive relations from kinetic theory for the collisional interspecies momentum exchange

$$\mathbf{R}_j=-n_j m_j\sum_{k\neq j} n\nu_{jk}(\mathbf{v}_j-\mathbf{v}_k) \tag{3}$$

and for the neoclassical parallel viscous force[10]

$$\mathbf{B}\cdot\nabla\cdot\pi_j=3\langle(\hat{n}\cdot\nabla B)^2\rangle\left[\frac{Rqn_j m_j v_{\mathrm{th}j}\nu^*_j}{(1+\nu^*_j)(1+\epsilon^{3/2}\nu^*_j)}\right]\frac{\mathbf{v}_j\cdot\mathbf{B}_\theta}{B_\theta^2}, \tag{4}$$

where $\nu^*_j\equiv\nu_{ij}qR/\epsilon^{3/2}v_{\mathrm{th}j}$. In the toroidal geometry approximation $\langle(\mathbf{n}\cdot\nabla B)^2\rangle=\frac{1}{2}(\epsilon/qR)^2B^2$, where $\epsilon=r/R$. The flux surface averaged toroidal component of the neoclassical viscous force consists of ''perpendicular'' and gyroviscous parts, with the latter being much larger in toroidal geometry. The first-principles neoclassical gyroviscous force acting on a given flux surface is[16]

$$\langle R^2\nabla\phi\cdot\nabla\cdot\pi_j\rangle=-\left\langle\frac{1}{Rh_\theta}\frac{\partial}{\partial l_\psi}\left(R^3h_\theta\eta_{4j}\frac{\partial(v_{\phi j}R^{-1})}{\partial l_\theta}\right)\right\rangle=\frac{1}{2}\tilde{\theta}_j G_j\frac{n_j m_j T_j}{e_j B}\frac{v_{\phi j}}{R}\equiv Rn_j m_j\nu_{dj}v_{\phi j}, \tag{5}$$

where l_ψ and l_θ are the length elements in the (radial) ψ and (poloidal) θ directions in flux surface coordinates. A standard right-hand coordinate system in flux surface (ψ,θ,ϕ) or toroidal (r,θ,ϕ) coordinates is used in this paper, where the positive ϕ direction is in the direction of the toroidal magnetic field, the positive θ direction is in the direction of the poloidal magnetic field created by a toroidal current in the same direction as the toroidal magnetic field, and the positive ψ direction is in the direction of the outward normal to the flux surfaces. The toroidal geometry approximation has been made in writing the last form of Eq. (5).

Assuming a low order Fourier expansion of the density, velocity, and potential variation over the flux surface, the poloidal asymmetry factor and the radial gradient factor on a given flux surface are given in the toroidal geometry approximation by

$$\begin{aligned}\tilde{\theta}_j&\equiv(4+\tilde{n}_j^c)\tilde{v}_{\phi j}^s+\tilde{n}_j^s(1-\tilde{v}_{\phi j}^c)\\&=(4+\tilde{n}_j^c)[-\hat{v}_{\theta j}(\hat{v}_{\phi j})^{-1}(\tilde{\Phi}^s+\hat{n}_j^s)+\tilde{\Phi}^s]\\&\quad+\tilde{n}_j^s[\hat{v}_{\theta j}(\hat{v}_{\phi j})^{-1}(2+\tilde{\Phi}^c+\tilde{n}_j^c)-\tilde{\Phi}^c]\end{aligned} \tag{6}$$

and

$$G_j(r)\equiv-\frac{r}{\eta_{4j}v_{\phi j}}\frac{\partial(\eta_{4j}v_{\phi j})}{\partial r}, \tag{7}$$

where $\hat{v}_{\phi j}\equiv v_{\phi j}/v_{\mathrm{th}j}$ and $\eta_{4j}=n_j m_j T_j/e_j B$.

In deriving Eq. (5) for the ''drag force'' acting over a flux surface, the poloidal variation of the density over the flux surface was expanded,

$$n_j(r,\theta)=n_j(r)(1+\epsilon(\tilde{n}_j^c\cos\theta+\tilde{n}_j^s\sin\theta)), \tag{8}$$

with a similar expansion for the toroidal velocity and the electrostatic potential Φ. This type of low order expansion is sufficient to describe the type of in–out and up–down asymmetries which we believe to be of the greatest importance for the development of this paper. The expansion could be extended to higher order in an obvious manner to treat higher m asymmetries, but this is not felt to be necessary.

B. Poloidal rotation and density asymmetries

Equations for the normalized poloidal rotation velocities on the flux surface, $\hat{v}_{\theta_j}\equiv v_{\theta_j}/\beta v_{\mathrm{th}_j}$ $(\beta\equiv B_\theta/B_\phi)$, and the cos and sin components of the density variations over the flux surface are developed[17] by using Eq. (8) in the poloidal projection of the momentum balance Eq. (2) and integrating over θ, with the weighting functions $\xi=1$, $\cos\theta$, and $\sin\theta$,

$$\left[q^2 f_j\left\{1+\frac{5}{6}\tilde{n}_j^c+2\tilde{n}_j^s+\frac{1}{3}(\tilde{n}_j^s)^2+\frac{1}{3}(\tilde{n}_j^c)^2+\frac{1}{2}\tilde{\Phi}^s\tilde{n}_j^s+\frac{1}{2}\tilde{\Phi}^c(5+\tilde{n}_j^c)\right\}+\sum_{k\neq j}\nu_{jk}^*-q^2\hat{v}_{\phi j}(\tilde{n}_j^s+\tilde{\Phi}^s)\right]\hat{v}_{\theta j}$$
$$=\hat{M}_{\theta j}+\hat{v}_{rj}+\sum_{k\neq j}\nu_{jk}^*\sqrt{\frac{m_j}{m_k}}\hat{v}_{\theta k}-q^2(\hat{v}_{\phi j})^2\tilde{\Phi}^s$$
$$-\tfrac{1}{2}q^2 f_j\hat{v}_{\phi j}[\tilde{\Phi}^s\tilde{n}_j^s+\tilde{\Phi}^c(5+\tilde{n}_j^c)], \tag{9}$$

$$\left[\left(\frac{2}{3}f_j-\beta^2\sum_{k\neq j}\nu_{jk}^*\right)\hat{v}_{\theta j}\right]\tilde{n}_j^s-\frac{1}{2}\tilde{n}_j^c$$
$$=-(\hat{v}_{\phi j})^2+\frac{1}{2}\hat{\Phi}_j\tilde{\Phi}^c-\beta^2\sum_{k\neq j}\nu_{jk}^*\hat{v}_{\theta j}\tilde{n}_k^s, \tag{10}$$

and

$$\left[\left(\frac{2}{3}f_j-\beta^2\sum_{k\neq j}\nu_{jk}^*\right)\hat{v}_{\theta j}\right]\tilde{n}_j^c+\frac{1}{2}\tilde{n}_j^s$$
$$=-f_j\hat{v}_{\theta j}-\frac{1}{2}\hat{\Phi}_j\overline{\Phi}^s+\beta^2\sum_{k\neq j}\nu_{jk}^*\left(\hat{v}_{\theta j}-\sqrt{\frac{m_j}{m_k}}\hat{v}_{\theta k}\right)$$
$$-\beta^2\sum_{k\neq j}\nu_{jk}^*\hat{v}_{\theta j}\tilde{n}_k^c-\beta^2\hat{v}_{rj}, \tag{11}$$

where v_{rj} is the radial velocity,

$$\hat{v}_{\theta j}\equiv v_{\theta j}/\beta v_{\mathrm{th}j},\quad \hat{v}_{\phi j}\equiv v_{\phi j}/v_{\mathrm{th}j},\quad \hat{v}_{rj}=\frac{v_{rj}}{\beta\delta_\theta v_{\mathrm{th}j}},$$
$$\hat{M}_{\theta j}\equiv\frac{M_{\theta j}}{n_j m_j\omega_j\beta v_{\mathrm{th}j}},\quad \hat{\Phi}_j\equiv\frac{e_j}{m_j}\frac{\Phi}{v_{\mathrm{th}j}^2},\quad \omega_j\equiv\frac{v_{\mathrm{th}j}}{qR}, \tag{12}$$

and

$$f_j\equiv\frac{\varepsilon^{-3/2}\nu_{jj}^*}{(1+\varepsilon^{-3/2}\nu_{jj}^*)(1+\nu_{jj}^*)}. \tag{13}$$

Note that the normalized collision frequencies $\nu_{jk}^*=\nu_{jk}/(qR/v_{\mathrm{th}j})$ differ from the normalized collision frequency $\nu^*{}_j=\nu_{jj}//(qR/v_{\mathrm{th}j})\varepsilon^{3/2}$ defined and used previously.

C. Radial electric field

The component of the radial electric field which is constant over the flux surface is obtained self-consistently from the flux surface averaged toroidal projection of the momentum balance equation summed over species.[10] At this point, we specialize the formalism to a main ion species ''i'' and an impurity species ''I'' in order to simplify. With this specialization, the radial electric field may be written

$$\frac{E_r}{B_\theta}=[\{\hat{\mu}_i+\hat{\mu}_I(1+\xi_i)\}\hat{M}_{\phi I}+\{\hat{\mu}_I+\hat{\mu}_i(1+\xi_I)\}\hat{M}_{\phi i}$$
$$+\{\beta_i+\beta_I(1+\xi_i)\}\hat{\mu}_I P_I'+\{\beta_I+\beta_i(1+\xi_I)\}\hat{\mu}_i P_I']/$$
$$[\hat{\mu}_i\{\beta_I+\beta_i(1+\xi_I)\}+\hat{\mu}_I\{\beta_i+\beta_I(1+\xi_i)\}], \tag{14}$$

where $M_{\phi j}$ is the normalized toroidal projection of the neutral beam (or other) momentum input on the given flux surface, P_j' is the normalized radial pressure gradient across the given flux surface, and

$$\hat{\mu}_j\equiv\frac{3/2\sqrt{\varepsilon}(\nu_{jj}/\nu_{jk})}{(1+\nu^*{}_j)(1+\varepsilon^{3/2}\nu^*{}_j)},\quad P_j'\equiv\frac{1}{n_j e_j B_\theta}\frac{\partial p_j}{\partial r},$$
$$\beta_j\equiv\frac{\nu_{dj}}{\nu_{jk}},\quad \xi_j\equiv\hat{\mu}_j+\beta_j,\quad \hat{M}_{\phi j}\equiv\frac{M_{\phi j}}{n_j m_j\nu_{jk}}. \tag{15}$$

D. Toroidal rotation

Equation (2) can now be solved for the impurity toroidal velocity on the flux surface,[10]

$$v_{\phi I}=\Big[\{M_{11i}+(1+\xi_i)M_{11I}\}-\{\hat{\mu}_I(1+\xi_i)P_I'+\hat{\mu}_i P_i'\}$$
$$+\{\hat{\mu}_I(1+\xi_i)+\hat{\mu}_i\}\left(\frac{E_r}{B_\theta}\right)\Big]\Big/[\xi_i(1+\xi_I)+\xi_I], \tag{16}$$

and for the (small) difference in main ion and impurity toroidal velocities,

$$v_{\phi i}-v_{\phi I}=[(\hat{\mu}_i+\hat{\mu}_I)(\beta_I\hat{M}_{11i}-\beta_i\hat{M}_{11I})$$
$$-\hat{\mu}_i\hat{\mu}_I(\beta_i+\beta_I)(P_i'-P_I')]. \tag{17}$$

E. Solution of rotation problem

Equations (9)–(11), (14), (16), and (17) must be solved simultaneously (or iteratively) for the poloidal and toroidal rotation velocities, the poloidal density asymmetries, and the radial electric field. Within the context of the two-species, multifluid equations and the constitutive relations of Eqs. (3)–(5), this set of equations defines a ''first-principles'' and internally self-consistent neoclassical calculation.

F. Transport fluxes

The toroidal component of the momentum balance equation for each species can be flux surface averaged to obtain an expression for the cross field (radial) transport flux $\Gamma_{rj}\equiv n_j\mathbf{v}_{rj}$,

$$\Gamma_j=\langle R^2\nabla\phi\cdot\nabla p_j\rangle+\langle R^2\nabla\phi\cdot\nabla\cdot\pi_j\rangle-\langle R^2\nabla\phi\cdot\mathbf{M}_j\rangle$$
$$+\langle R^2\nabla\phi\cdot(n_j m_j(\mathbf{v}_j\cdot\nabla)\mathbf{v}_j)\rangle+\langle R^2\nabla\phi\cdot n_j e_j\nabla\Phi\rangle$$
$$-\langle R^2\nabla\phi\cdot\mathbf{R}_j\rangle. \tag{18}$$

Using the previous expressions for the toroidal rotation velocity, this expression for the radial impurity flux may be written in a form that associates various terms with conventional neoclassical fluxes or with one of the various effects discussed previously:

$$\Gamma_I\equiv\Gamma_I^{\mathrm{PS}}+\Gamma_I^{\mathrm{nc}}+\Gamma_I^M+\Gamma_I^I+\Gamma_I^{\Phi'}+\Gamma_I^{\tilde{\Phi}}. \tag{19}$$

Explicit expressions for the various terms in Eq. (19) are given in the following in the ''two-species'' approximation. The value of B_θ is positive or negative depending on whether the toroidal current is parallel or antiparallel, respectively,

with the toroidal magnetic field, and the value of M_ϕ or $M_\parallel$ is positive or negative depending on whether the beam injection direction is parallel or antiparallel, respectively, to the toroidal magnetic field.

The first two terms correspond to the Pfirsch–Schluter and ''neoclassical'' fluxes of conventional neoclassical theory

$$\Gamma_I^{\rm PS}=\frac{n_I m_I \nu_{Ii}\varepsilon^2}{e_I B_\theta}\left[\left\{\left(\frac{1+2q^2}{q^2}\right)+\tilde{n}_i^c\right\}P_i' - \left\{\left(\frac{1+2q^2}{q^2}\right)+\tilde{n}_I^c\right\}(1+\beta_I)P_I'\right] \tag{20}$$

and

$$\Gamma_I^{\rm nc}=\frac{n_I m_I \nu_{Ii}}{e_I B_\theta d}[\{\hat{\mu}_i\hat{\mu}_I+\varepsilon^2\hat{\mu}_i((1+\beta_I)\tilde{n}_I^c-\tilde{n}_i^c)\}P_i' - \{\hat{\mu}_I(\xi_i+\beta_I(1+\xi_i))+\varepsilon^2\hat{\mu}_I(\tilde{n}_i^c-\tilde{n}_I^c)\}P_I'], \tag{21}$$

where

$$d\equiv\xi_i+\xi_I(1+\xi_i). \tag{22}$$

For a negative main ion pressure gradient ($P_i'<0$), these fluxes are generally inward for impurities and outward for main ions. The corresponding main ion transport fluxes are given by similar expressions with the i and I subscripts interchanged.

The third flux component in Eq. (19) is the contribution resulting directly from momentum exchange between beam ions and plasma and impurity ions,

$$\Gamma_I^M=-\frac{n_I m_I \nu_{Ii}}{e_I B_\theta d}\times[\hat{M}_{\phi I}\{\hat{\mu}_I(1+\xi_i)+\varepsilon^2(d+(1+d)\tilde{n}_I^c-(1+\xi_i)\tilde{n}_i^c)\} + \hat{M}_{\phi i}\{\hat{\mu}_I+\varepsilon^2((1+\tfrac{1}{2}(\beta_I+\xi_I))\tilde{n}_I^c-\tilde{n}_i^c)\}]. \tag{23}$$

The corresponding main ion flux component is given by a similar expression with i and I interchanged. Both the impurity and main ion fluxes are generally inward for co-injection ($M_\phi>0$) and outward for counterinjection ($M_\phi<0$), when the toroidal current is in the same direction as the toroidal magnetic field, and conversely when the toroidal current and magnetic field are antiparallel.

The fourth flux component in Eq. (19) results from the inertial ($nm(\mathbf{v}\cdot\nabla)\mathbf{v}$) term in the momentum balance equation, which produces $O(\varepsilon^2)$ terms in the rotation velocities which in turn contribute an $O(\varepsilon^2)$ flux component

$$\Gamma_I^I=-\frac{n_I m_I \nu_{Ii}\varepsilon^2 B_\phi}{e_I B_\theta B^2 d}[(\xi_i+\beta_I(1+\xi_i))\langle\hat{G}_I\rangle-\hat{\mu}_I\langle\hat{G}_i\rangle], \tag{24}$$

where

$$\langle\hat{G}_I\rangle\equiv\frac{1}{2}\left(\frac{B_\phi}{qR\nu_{Ii}}\right)\left[\left\{\left(\frac{B_\phi}{B_\theta}v_{\theta I}\right)^2+w^2+2\delta_1 w\right\}\tilde{n}_I^s + \{2\delta_2 w\}\tilde{n}_i^s\right] \tag{25}$$

and

$$\delta_1\equiv\frac{(\alpha/z_I)}{(1+(\alpha/z_I))e_i B_\theta}\left[\frac{1}{n_I}\frac{\partial p_I}{\partial r}-\frac{T}{(1+(\alpha/z_I))}\times\left\{\left(\frac{\alpha}{z_I}\right)\frac{1}{n_I}\frac{\partial n_I}{\partial r}+\frac{1}{n_i}\frac{\partial n_i}{\partial r}\right\}\right], \tag{26a}$$

$$\delta_2\equiv\frac{1}{(1+(\alpha/z_I))e_i B_\theta}\left[\frac{1}{n_i}\frac{\partial p_i}{\partial r}-\frac{T}{(1+(\alpha/z_I))}\times\left\{\frac{1}{n_I}\frac{\partial n_I}{\partial r}+\frac{1}{n_i}\frac{\partial n_i}{\partial r}\right\}\right], \tag{26b}$$

and

$$w_j\equiv P_J'-\frac{E_r}{B_\theta}. \tag{27}$$

The expression for $\langle G_I\rangle$ is obtained from Eq. (25) by interchanging i and I subscripts and interchanging δ_1 and δ_2. The corresponding transport flux component for main ions is obtained by interchanging i and I in Eq. (24).

The fifth term describes the radial impurity flux that is driven directly by the radial electric field

$$\Gamma_I^{\Phi'}=\frac{n_I m_I \nu_{Ii}}{e_I B_\theta}\left[\hat{\mu}_I\gamma_I+\varepsilon^2\left\{\beta_I\left(\frac{1+2q^2}{q^2}\right) + (\beta_I+\gamma_I)\tilde{n}_I^c-\gamma_I\tilde{n}_i^c\right\}\right]\left(\frac{E_r}{B_\theta}\right), \tag{28}$$

where

$$\gamma_I\equiv\frac{\beta_i+\beta_I(1+\xi_i)}{\xi_i+\xi_I(1+\xi_i)}. \tag{29}$$

The corresponding main ion flux component is obtained by interchanging I and i. This flux component will generally have the same sign as the radial electric field (i.e., outward for $E_r>0$). Since E_r tends to be positive for injection parallel to the toroidal current and negative for injection antiparallel to the toroidal current, this flux component would be expected to have a corresponding behavior.

The last term in Eq. (19) is the impurity transport driven by the poloidal variation in the electrostatic potential over the flux surface, is of $O(\alpha/Z_I)$, and can usually be neglected. An explicit expression for this term is given in Ref. 10.

The net impurity flux depends upon a competition among different flux components and may be inward or outward, depending on the specific operating conditions.

G. Temperature screening correction

Up to this point, the formalism is internally self-consistent and ''first principles'' within the context of the multifluid Eqs. (1) and (2), the constitutive relations of Eqs. (3) and (4), and the neoclassical expression for the gyroviscosity of Eq. (5). However, the constitutive relation of Eq. (3) neglects thermal friction, which makes an important contribution to ''temperature screening'' of impurities, i.e., to reducing or reversing the inward $\Gamma_I^{\rm PS}$ and $\Gamma_I^{\rm nc}$. Since there is

evidence of temperature screening in recent DIII-D experiments,[20] we will correct these two components of the transport flux to account for thermal friction.

Rutherford's expression[21] for the neoclassical Pfirsch–Schluter impurity flux in a collisional plasma is

$$\Gamma_I^{\mathrm{PS}}=-\left(\frac{1+2q^2}{q^2}\right)\frac{n_I m_I \nu_{Ii}\varepsilon^2}{e_I B_\theta}\left[\left(c_I+\frac{c_2^2}{c_3}\right)(P_I'-P_i')-\frac{5}{2}\frac{c_2}{c_3}\frac{1}{e_I B_\theta}\frac{\partial T}{\partial r}\right], \tag{30}$$

where

$$c_I+\frac{c_2^2}{c_3}=0.47+\frac{0.35}{0.66+\alpha_I},\qquad \frac{5}{2}\frac{c_2}{c_3}=0.30+\frac{0.41}{0.58+\alpha_I},\quad \alpha_I=\left(\frac{z_I}{z_i}\right)^2\frac{n_I}{n_i}. \tag{31}$$

Since Rutherford did not consider the effect of poloidal density asymmetries, we correct our expression for the Pfirsch–Schluter flux by multiplying Eq. (20) by the factor (c_1+c_{22}/c_3) and adding a term

$$\Delta\Gamma_I^{\mathrm{PS}}=\left(\frac{1+2q^2}{q^2}\right)\frac{n_I m_I \nu_{Ii}\varepsilon^2}{e_I B_\theta}\frac{5}{2}\frac{c_2}{c_3}\frac{\partial T}{\partial r}. \tag{32}$$

We use the Hinton–Hazeltine results[6] for a two-species plasma with both species in the plateau regime to construct an additive correction to Eq. (21) to account for thermal friction

$$\Delta\Gamma_I^{\mathrm{nc}}=-\frac{n_I m_I \nu_{Ii}}{z_I B_\theta^2}\left(\frac{2\varepsilon^{1/2}K_{11}^I}{F_{Ii}}\right)\left[\frac{1}{z_i}\left(\frac{5}{2}-\frac{K_{12}^i}{K_{11}^i}\right)-\frac{1}{z_I}\left(\frac{5}{2}-\frac{K_{12}^I}{K_{11}^I}\right)\right]\frac{\partial T}{\partial r}, \tag{33}$$

where

$$K_{11}^I=\frac{0.73(1+0.53/\alpha_I)}{1+1.26\nu_{*I}'(1+0.53/\alpha_I)},\qquad K_{12}^I=\frac{0.73(1+0.71/\alpha_I)}{1+0.37\nu_{*I}'(1+0.71/\alpha_I)},$$
$$F_{Ii}=1+\left(\frac{2m_I}{m_i}\right)^{1/2}K_{11}^I/\alpha_I K_{11}^i,\qquad \nu_{*I}'=\frac{\sqrt{2}rB\nu_{Ii}}{B_\theta v_{\mathrm{th}_i}\varepsilon^{3/2}},\quad \nu_{*i}'=\left(\frac{z_i}{z_I}\right)^2\frac{\nu*'_I}{\sqrt{2}}. \tag{34}$$

The corrections for the main ion fluxes are obtained by interchanging the i and I subscripts.

III. COMPUTATIONAL MODEL

Certain simplifications are made in implementing the theoretical model of Sec. II for computations. Toroidal geometry is assumed, and radial profiles are assumed to be representable by a parabola to a power on a pedestal.

$$x(r)=(x_0-x_{\mathrm{ped}})\left(1-\left(\frac{r}{a}\right)^2\right)^{\alpha_x}+x_{\mathrm{ped}}. \tag{35}$$

Specifying the radial shape in this manner allows the toroidal rotation velocity to be calculated from an overall angular momentum balance on the plasma[22]

$$\Gamma_\phi=\frac{(2\pi R)\int_0^a\langle R\Sigma_j^{\mathrm{ions}}n_j m_j v_{\phi j}\rangle 2\pi r\,dr}{\tau_\phi^{\mathrm{th}}}, \tag{36}$$

where the beam torque is given in terms of beam power (P_b), particle energy (E_b), and mass (m_b) by

$$\Gamma_\phi=\sqrt{\frac{2m_b}{E_b}}P_b R_{\tan}, \tag{37}$$

where $R_{\tan}$ is the beam tangency radius, and the theoretical (gyroviscous) angular momentum confinement time is defined

$$\tau_\phi^{\mathrm{th}}\equiv\frac{\Sigma_j^{\mathrm{ions}}\int_0^a\langle Rn_j m_j v_{\phi j}\rangle r\,dr}{\Sigma_j^{\mathrm{ions}}\int_0^a\langle R^2\nabla\phi\cdot\nabla\cdot\pi_j\rangle r\,dr}=\frac{\int_0^a R\left(\sum_j^{\mathrm{ions}}\frac{n_j}{n_e}m_j\right)n_e v_\phi r\,dr}{\int_0^a\frac{1}{2}R^{-1}\frac{T}{eB}\left(\sum_j^{\mathrm{ions}}\frac{n_j}{n_e}\frac{m_j}{z_j}\tilde{\theta}_j G_j\right)n_e v_\phi r\,dr}$$
$$=\left(\frac{R^2eB}{T_0}\right)\left(\frac{h_{nvT}}{h_{nv}}\right)\times\frac{\left(\sum_j^{\mathrm{ions}}\frac{n_j}{n_e}m_j\right)}{\left(\sum_j^{\mathrm{ions}}\frac{n_j}{n_e}\frac{m_j}{z_i}\tilde{\theta}_j r(L_{nj}^{-1}+L_{Tj}^{-1}+L_{v\phi j}^{-1})\right)_{\mathrm{av}}}. \tag{38}$$

In going from the first to second expression in Eq. (38) a common temperature and toroidal rotation velocity were assumed for all ions, and in going to the final expression the ( ) terms in numerator and denominator were replaced with average values (obtained in this paper by evaluating the expressions at $r/a=\frac{1}{2}$), which enabled the radial integrals to be performed analytically. The quantities h_{nv} and h_{nvT} are normalized radial volume integrals of the products of the radial profiles of the quantities indicated by the subscripts [see Eq. (16) of Ref. 4] and are given by

$$h_{nv}=1+\alpha_n+\alpha_v,\qquad h_{nvT}=1+\alpha_n+\alpha_v+\alpha_T, \tag{39}$$

when $n_{\mathrm{ped}}=v_{\mathrm{ped}}=T_{\mathrm{ped}}=0$ and by somewhat more complicated expressions when the pedestal values are finite. Using the same type of approximation, Eq. (36) can be solved for the central toroidal rotation frequency

$$\Omega_{\phi 0}^{\mathrm{th}}=\frac{v_{\phi 0}^{\mathrm{th}}}{R}=\frac{\Gamma_\phi\tau_\phi^{\mathrm{th}}h_{nv}}{2\pi^2a^2R^3\left(\sum_j^{\mathrm{ions}}\frac{n_j}{n_e}m_j\right)_{\mathrm{av}}n_{e0}}. \tag{40}$$

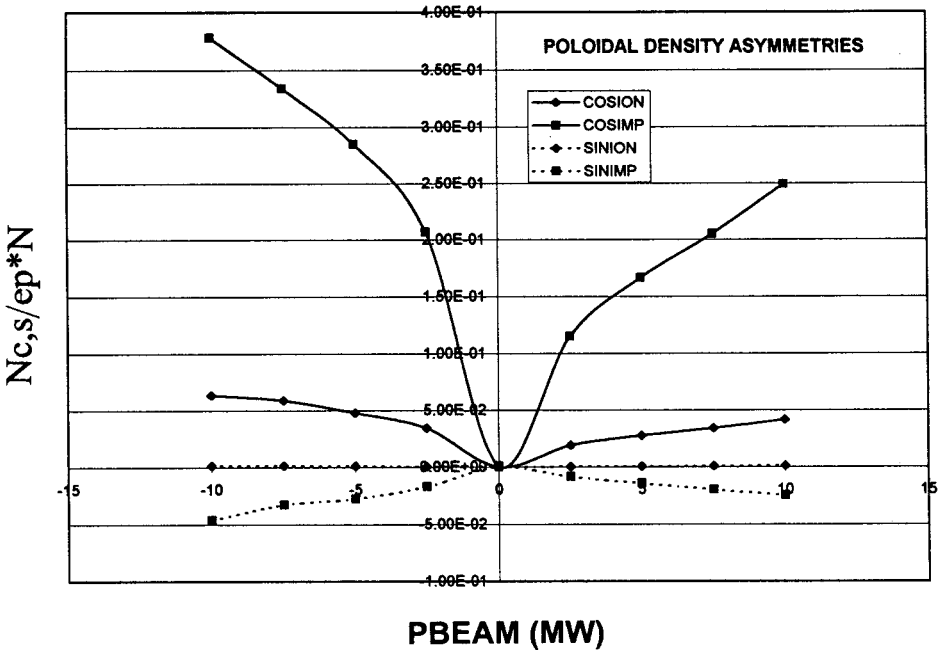

FIG. 1. Poloidal density asymmetries at $r/a=0.5$ in model problem calculation.

Conversely, if the central toroidal rotation frequency is measured, then the experimental angular momentum confinement time can be constructed from

$$\tau_\phi^{\exp}=\frac{2\pi^2a^2R^3\left(\sum_j^{\text{ions}}\frac{n_j}{n_e}m_j\right)_{\text{av}}n_{e0}\Omega_{\phi0}^{\exp}}{\Gamma_\phi h_{nv}}. \tag{41}$$

In the same spirit, the radial electric field can be calculated directly from momentum balance using the toroidal rotation velocity obtained from solving Eq. (36) using the radial shapes of Eq. (35),

$$\frac{E_r}{B_\theta}=P_j'+v_{\phi j}-\frac{B_\phi}{B_\theta}v_{\theta j}. \tag{42}$$

In order to evaluate the transport fluxes on a given flux surface, it is necessary to calculate the beam toroidal (M_ϕ) and parallel ($M_\parallel$) momentum deposition rate densities on the flux surface. For our purposes in this paper, we use the simple model

$$M_\phi(r)=\frac{J_0M_b}{(2\pi r)\lambda_0}\sum_{j=1}^{4}\frac{e^{-l_{\sigma j}/\lambda_0}\cos\chi_j}{2\pi R_j}, \tag{43}$$

where

$$J_0=\frac{P_b}{E_b},\quad M_b=\sqrt{2m_bE_b},\quad \lambda_0=\frac{5.5\times10^{17}E_b}{A_bn_{e0}Z_{\text{eff}}^{1/2}}, \tag{44}$$

where P_b, E_b, and A_b are the beam power, energy per particle, and atomic mass of the beam particle.

The beam may cross the flux surface at minor radius r as many as four times. The $l_{\sigma j}$ are the distances along the beam trajectory from where it enters the plasma to the jth crossing of the flux surface at r, χ_j is the angle between the beam direction and the positive toroidal direction at the jth crossing, and $R_j=R_0\pm r$ is the value of R at the jth crossing.

We note that the simplifications of this section are made to obtain a more tractable computational model for our present purposes and are not an intrinsic part of the theoretical model described in Sec. II.

IV. MODEL PROBLEM CALCULATIONS

In this section we present the results of some model problem calculations intended to illustrate the features of the theory presented in previous sections. For this purpose, we choose a model problem typical of DIII-D ($R=1.7$ m, $a=0.60$ m, $\kappa=1.7$, $Z_{\text{eff}}=1.5$ with carbon, $n_{e0}=5E19$, $T_0=12.5$ keV, $\alpha_n=0.1$, $\alpha_T=2.2$, $\alpha_v=2.9$, $B_t=2.1$ T, $I=1.3$ MA) and carry out a series of calculations for different injected beam power levels and directions and current directions. (We will denote injection and current directions aligned with B_t as positive and directions opposite to B_t as negative.) Note that the temperature and density were held constant as the beam injection power changed in these model problems, contrary to the situation that would obtain in an actual experiment. The results of these calculations are given in Figs. 1–5.

The sine and cosine components of the poloidal density asymmetries for carbon impurities (COSIMP, SINIMP) and deuterium main ions (COSION, SINION) and the poloidal rotation velocities for the impurities and main ions are shown in Figs. 1 and 2 as a function of neutral beam injection power. These results are for the current antiparallel to $B_t(I<0)$. Clearly, the density asymmetries and the poloidal rotation velocities increase in magnitude as the magnitude of the injected beam power (and the magnitude of the toroidal rotation velocity) increases. The results for the current parallel to $B_t(I>0)$ differed only slightly from those shown in Figs. 1 and 2, except that the sine component of the impurity density is positive and the sine component of the main ion density is negative when $I>0$—just the opposite of the situ-

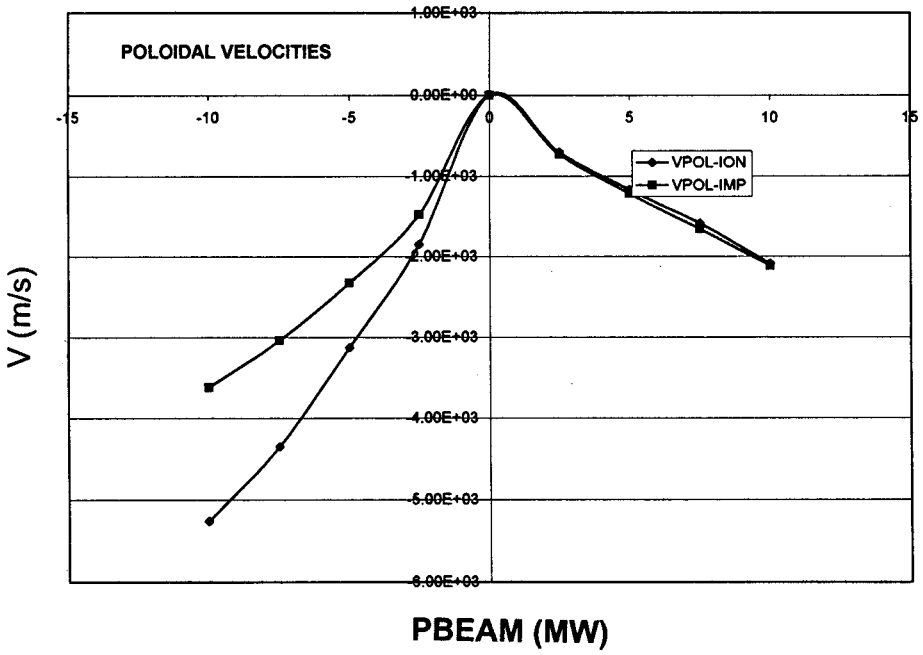

FIG. 2. Poloidal rotation velocities at $r/a=0.5$ in model problem calculation.

ation shown in Fig. 1. This difference in the sine components of the densities leads to a difference in the gyroviscous momentum transfer, which leads to a difference in the magnitude of the toroidal rotation velocity. The slight difference in toroidal rotation velocities for $I>0$ and $I<0$ is shown in Fig. 3.

The radial electric field is reversed when the current direction is reversed, as shown in Fig. 3. This difference in sign of the radial electric field causes a difference in sign of the radial electric field component of the transport flux given by Eq. (28). In addition, the difference in current direction results in a difference in the sign of B_θ, which results in a difference in direction of the momentum and inertial transport fluxes of Eqs. (23) and (24).

The various components of the transport flux for the main ions and impurities are shown for the case $I<0$ in Figs. 4 and 5. The total transport fluxes are shown for both $I<0$ and $I>0$. The total transport fluxes are essentially the Pfirsh–Schluter flux for the impurities ($\nu_{II}^*=0.026$) and the neoclassical flux for the main ions ($\nu_{ii}^*=0.0011$), in both cases modified somewhat by the other transport fluxes, which tended to cancel each other out. In the $I>0$ case, the

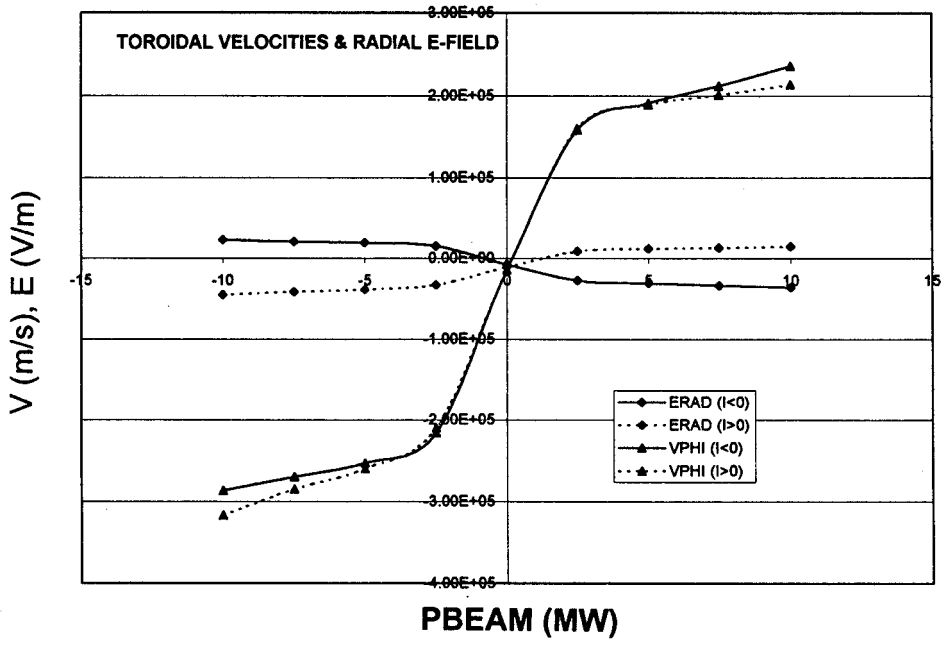

FIG. 3. Toroidal rotation velocities and radial electric field at $r/a=0.5$ in model problem calculation.

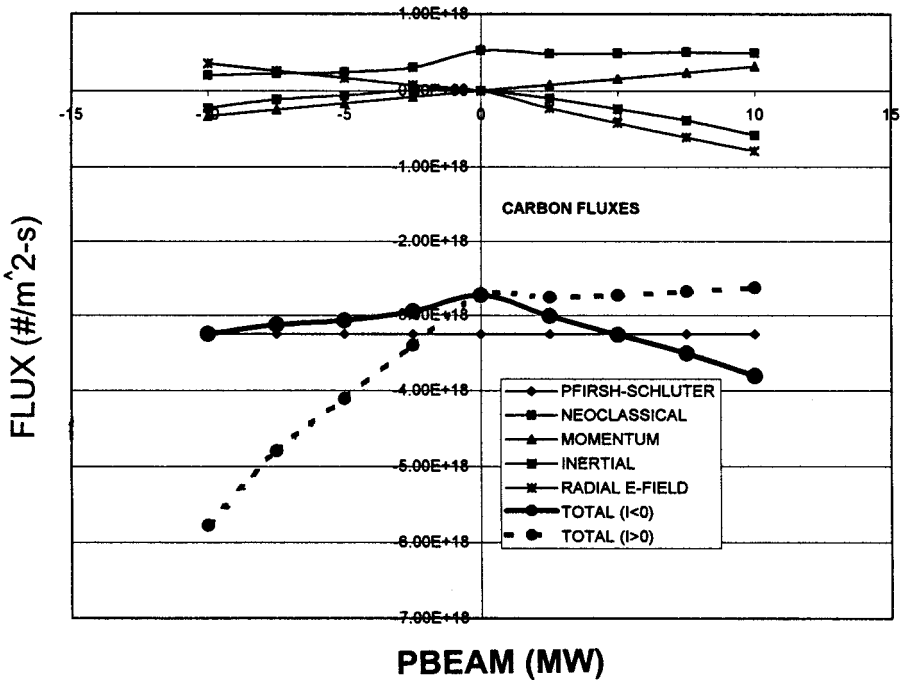

FIG. 4. Carbon radial transport fluxes at $r/a=0.5$ in model problem calculation.

inertial impurity flux of Eq. (24) was large and negative for large negative P_b and became positive for positive P_b, accounting for the reduction in the magnitude of the inward (negative) impurity flux as the beam injected power changed from strongly negative to strongly positive, reminiscent of the previous finding[10] that $P_b<0$ led to greater central impurity accumulation than $P_b>0$. The impurity toroidal Mach number <0.75 at the $r/a=0.5$ location where the fluxes were calculated in this model problem. More dramatic modification of the pressure-driven Pfirsh–Schluter and neoclassical fluxes by the other ''rotational'' flux components would be expected if Mach-one conditions were approached or exceeded.

V. COMPARISON WITH EXPERIMENT

It is not our purpose in this paper to provide a broad application of the theory to interpretation of experiment. An investigation of this topic is in progress and will be the subject of future papers.

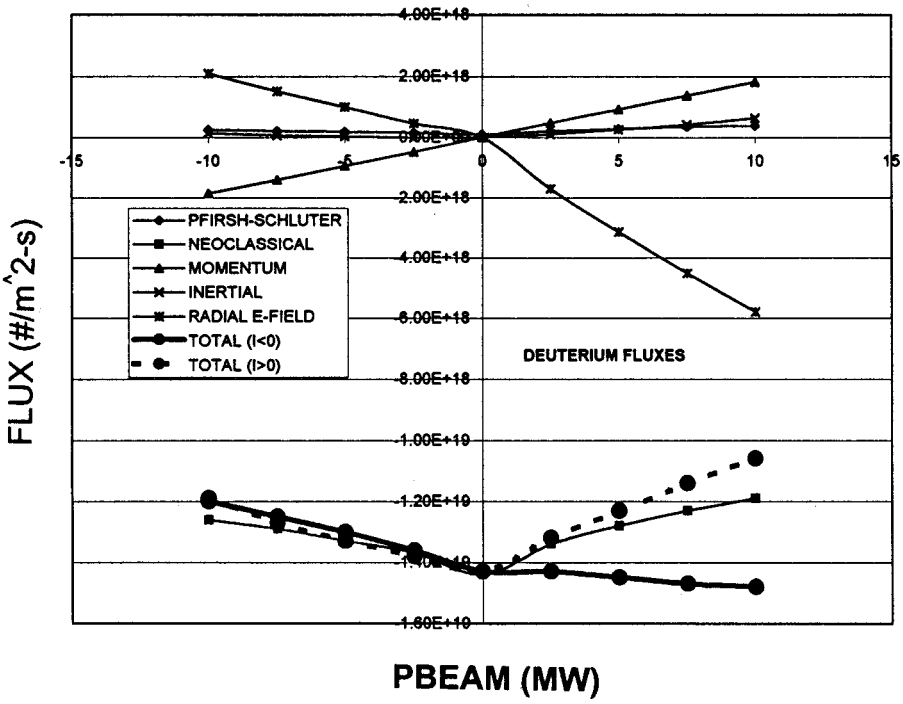

FIG. 5. Deuterium radial transport fluxes at $r/a=0.5$ in model problem calculation.

However, it is useful to at least touch base with experiment in order to provide some measure of confidence in the theoretical formalism. Since a central feature of the formalism is the self-consistent neoclassical calculation of rotation, we calculated the central rotation frequency in a well-documented[23,24] DIII-D deuterium plasma *L*-mode shot (No. 98777 at 1.6 s) with a carbon impurity and $Z_{\rm eff}=1.5$. We used measured central values $v_{\phi 0}/R=0.75e5/\mathrm{s}$, $n_{e0}=4.3e19\,\mathrm{m}^{-3}$, $T_{i0}=3.5\,\mathrm{keV}$ and fit the measured radial profiles with Eq. (35) with $n_{\rm ped}=T_{\rm ped}=v_{\rm ped}=0.0$. The $(\,)_{\rm av}$ quantities were evaluated by solving for the poloidal velocity and poloidal density asymmetries at $r/a=\frac{1}{2}$, using the measured densities and temperature and the calculated toroidal rotation velocity at that radial location. The calculated central toroidal rotation frequency and angular momentum confinement time were $0.84E5/\mathrm{s}$ and 75 ms, which compare well with the corresponding experimental values of $0.75E5/\mathrm{s}$ and 62 ms, respectively. The ''experimental'' momentum confinement time was calculated with Eq. (41), using the abovementioned experimental parameters.

We note that momentum transport is widely regarded to be anomalous, because neoclassical perpendicular momentum transport has been found many times to be too small to account for measured momentum confinement times. However, the neoclassical gyroviscous momentum transport has been found[4] to be of the proper magnitude to account for measured momentum confinement times in a few tokamak experiments, and we find this once again.

We further note that the discharge that we considered in this section is considered to be highly turbulent, and that turbulent transport mechanisms are generally considered to be responsible for the thermal and particle transport.[23] It is thus perhaps somewhat surprising that a neoclassical model correctly predicts the momentum transport. However, momentum transport concerns ions exclusively, whereas the thermal transport probably has a large electron component. Investigation of this question is beyond the intended scope of this paper, but is being pursued as a separate issue.

VI. SUMMARY

A self-consistent, first-principles neoclassical theory for rotation and impurity transport in tokamaks is presented. The model consists of coupled calculations for the toroidal rotation speeds, the poloidal rotation speeds, and the asymmetries in the densities and potential over the flux surface, followed by a calculation of the radial electric field and the neoclassical particle fluxes for main ions and an impurity species. The calculation of particle fluxes takes into account inertial and radial electric field effects, direct beam-ion momentum exchange effects, and cross-field momentum transport effects, as well as the usual neoclassical collisional, parallel viscous, and thermal friction effects.

The implications of this theory for impurity transport in a tokamak are illustrated by a model problem calculation. The model problem calculations illustrate the importance of the relative directions of the magnetic field, current, and beam injection on radial particle fluxes of main ions and impurities.

[1] D. Meade and the TFTR Group, *Plasma Physics and Controlled Nuclear Fusion Research 1990* (IAEA, Vienna, 1991), Vol. I, p. 9.
[2] F. M. Levinton, M. C. Zarnstorff, S. H. Batha *et al.*, Phys. Rev. Lett. **75**, 4417 (1995).
[3] E. J. Strait, L. L. Lao, M. E. Mauel *et al.*, Phys. Rev. Lett. **75**, 4421 (1995).
[4] W. M. Stacey and D. R. Jackson, Phys. Fluids B **5**, 1828 (1993).
[5] R. Giannella, K. Behringer, B. Denne *et al.*, *Proceedings of the 16th European Conference on Controlled Fusion and Plasma Physics* (European Physical Society, Petit-Lancy, Switzerland, 1989), Vol. I, p. 209.
[6] F. L. Hinton and R. D. Hazeltine, Rev. Mod. Phys. **48**, 239 (1976).
[7] T. Ohkawa, Kaku Yugo Kenkyu, Bessatsu **32**, 1 (1974).
[8] W. M. Stacey and D. J. Sigmar, Phys. Fluids **22**, 2000 (1979); Nucl. Fusion **19**, 1665 (1979).
[9] K. H. Burrell, T. Ohkawa, and S. K. Wong, Phys. Rev. Lett. **47**, 511 (1981).
[10] W. M. Stacey and D. J. Sigmar, Phys. Fluids **27**, 2076 (1984); W. M. Stacey, A. W. Bailey, D. J. Sigmar, and K. C. Shaing, Nucl. Fusion **25**, 463 (1985).
[11] R. C. Isler, E. C. Crume, D. E. Arnurius *et al.*, Phys. Rev. Lett. **47**, 333 (1981).
[12] R. C. Isler, L. E. Murray, E. C. Crume *et al.*, Nucl. Fusion **23**, 1017 (1983).
[13] S. Suckewer, E. Hinnov, D. Hwang *et al.*, Nucl. Fusion **21**, 981 (1981).
[14] S. Suckewer, A. Cavallo, S. Cohen *et al.*, Nucl. Fusion **24**, 815 (1984).
[15] W. M. Stacey and M. A. Malik, Nucl. Fusion **29**, 937 (1989).
[16] W. M. Stacey and D. J. Sigmar, Phys. Fluids **28**, 2800 (1985).
[17] W. M. Stacey, Phys. Fluids B **4**, 3302 (1992).
[18] S. P. Hirshman and D. J. Sigmar, Nucl. Fusion **21**, 1079 (1981).
[19] W. A. Houlberg, K. C. Shaing, S. P. Hirshman, and M. C. Zarnstorff, Phys. Plasmas **4**, 3230 (1997).
[20] M. R. Wade, W. A. Houlberg, and L. Baylor, Phys. Rev. Lett. **84**, 282 (2000).
[21] P. H. Rutherford, Phys. Fluids **17**, 1782 (1974).
[22] W. M. Stacey, Nucl. Fusion **31**, 31 (1991).
[23] G. McKee, K. Burrell, R. Fonck *et al.*, Phys. Rev. Lett. **84**, 1922 (2000).
[24] M. Murakami, ORNL (private communication) (presentation to RI-mode workshop, 1999).